Periodic Robust Control of a Wind Turbine

Felix Biertümpfel * and Harald Pfifer †
Technische Universität Dresden, 01307 Dresden, Germany

Sabine Wisbacher ‡ and Daniel Ossmann§
Munich University of Applied Sciences HM, 80335 Munich, Germany

The increasing size of modern wind turbines leads to increased structural loads caused by effects such as turbulence or interactions between the rotor and tower structure. A common approach to alleviate out-of-plane structural loads in wind turbine control is the use of individual pitch control (IPC). IPC is frequently designed based on a linear time-invariant model, which is derived from averaging the dynamics over one rotational period. Wind turbine dynamics are, however, inherently time-periodic. Hence, this paper proposes the direct design of a periodic robust controller. The controller is designed through classical mixed sensitivity synthesis for optimal induced L_2 performance. A novel, structured, observer-based approach is used to simplify the synthesis problem by consecutively solving two periodic Riccati differential equations. Additionally, this leads to a highly structured controller that simplifies implementation on the hardware. To provide a realistic application of the proposed method, a controller was designed for a utility-scale 2.5 MW Liberty research turbine. Its stability and performance were verified using a high-fidelity nonlinear simulation and compared to baseline controllers, which were directly obtained from the manufacturer.

I. Introduction

The demand for larger wind turbines is already apparent and expected to continue, as recent market studies have highlighted (see [1]). Though upscaling brings benefits such as increased efficiency, cost-effectiveness, and overall higher energy production, it also results in elevated structural stresses. The augmented rotor size makes the blades more susceptible to turbulence and self-induced loads caused by interactions between the rotor and tower structure. Consequently, capitalizing on the benefits of larger wind turbines increasingly depends on advanced control techniques to mitigate these structural loads. State-of-the-art utility-scale wind turbines incorporate controllable components such as torque-varying generators, yaw-adjusting nacelles, and pitch-controlled blades. While collective blade pitching is usually used to maintain constant rated power in varying wind conditions, individual pitching additionally enables control strategies for load reductions. This Individual Pitch Control (IPC) is used to dampen out-of-plane oscillations on the blades and was first introduced by [2]. Since then, it has gained considerable popularity in the wind community. For instance, IPC with proportional-integral control achieved substantial load reduction during a field study by [3] on two- and three-bladed turbines. Similarly, a field study by [4, 5] reported even more significant load reduction on a utility-scale wind turbine using robust control-based IPC.

Most IPC controllers in literature share one common disadvantage. They are based on linear time-invariant (LTI) approximations of the wind turbine dynamics. In short, a so-called multi-blade coordinate (MBC) transformation as described in [6] is applied to the set of linearized models around a single rotor rotation, followed by a subsequent averaging over all these transformed models. Due to the averaging, the resulting LTI model does not accurately capture the inherently time-periodic behaviour of wind turbine dynamics anymore. In other words, important information on the dynamics is lost during the transformation process. While linear model-based controllers using MBC transformation commonly provide adequate performance, accurately using the periodic nature of wind turbines in the control design offers a path to further improvements. For example, in [7] and [8], a significant reduction in vibrations of four-bladed rotor systems has already been achieved using periodic linear quadratic regulators (LQR) and linear quadratic Gaussian (LQG) controllers compared to time-invariant control schemes. Similar, in [9], periodic LQG control has been applied to

*Postdoctoral Associate, Chair of Flight Mechanics and Control, felix.biertuempfel@tu-dresden.de
†Professor, Chair of Flight Mechanics and Control, harald.pfifer@tu-dresden.de
‡Research Assistant, Department of Mechanical, Automotive and Aeronautical Engineering, sabine.wisbacher@hm.edu
§Professor, Department of Mechanical, Automotive and Aeronautical Engineering, daniel.ossmann@hm.edu, AIAA Senior Member

utility scale research wind turbine and showcased a significant reduction in the out-of-plane bending moments. However, LQG control provides no robustness guarantees and suffers from an non-intuitive tuning process.

This paper contributes a systematic, periodic induced L_2 control design framework for rotor speed tracking and load reduction. It draws its inspirations from successful mixed sensitivity applications for control of flexible structures in the time invariant [10] and parameter varying case [11]. In the framework, specific dynamic modes are incorporated as performance measures. The extension of those results to periodic systems is based on the recent results on time varying control synthesis, see [12]. Section II introduces the periodic induced L_2 control synthesis and formulates the control design problem in a standard mixed sensitivity framework. Within this framework, the objective of adding damping to a specific mode is expressed as reducing peaks in the frequency response of a closed-loop transfer function. The closed-loop shaping approach further allows augmentation of the controller with roll-off and washout filters such that the control activity can be precisely confined to specific frequency ranges. Doing so avoids undesired interaction with unmodeled or uncertain plant dynamics at high frequencies. The proposed control design strategy is applied to a utility scale 2.5 MW Clipper wind turbine, as described in Section III. This section highlights the intuitive and strictly physically motivated choice of the weighting filters and scaling factors for the controller design. For a fixed, rated wind speed condition, a gridded linear time-periodic description of the wind turbine is derived using the *Fatigue, Aerodynamics, Structure and Turbulence* (FAST) software, which builds the basis of the control synthesis. A thorough verification is conducted in Section IV with the nonlinear simulation environment FAST using realistic, turbulent wind inputs. A manufacturer specified controller featuring proportional-integral collective blade-pitch control (CPC) together with a classical, double single-input single-output integral IPC controller (successfully field tested [4]) serve as the baseline for the verification. From time domain simulations using realistic turbulence models, damage equivalent loads are calculated and statistically analyzed. These analyses quantify the load reduction capabilities of the novel approach.

II. Robust Linear Time-Periodic Controller Design

Linearizing a time-periodic nonlinear system provides a linear time-periodic system P of the general form:

$$\left[\begin{array}{c} \dot{x}(t) \\ \hline y(t) \end{array}\right] = \left[\begin{array}{c|c} A(t) & B(t) \\ \hline C(t) & D(t) \end{array}\right] \left[\begin{array}{c} x(t) \\ \hline u(t) + d(t) \end{array}\right]. \tag{1}$$

The system matrices are functions of time with period T, i.e., $A(t) = A(t + kT)$ for all integers $k > 0$ and compatible size-wise to the corresponding vectors, e.g., $A(t) \in \mathbb{R}^{n_x \times n_x}$. The explicit time dependence will be omitted regularly to shorten the notation. In the course of the paper, the notation $y = Pu$ is used to state the input-output map defined by the state space representation (1) for zero initial conditions.

The performance of an LTP system can be specified in terms of its induced L_2 norm

$$\|P\| := \sup_{\substack{[u+d]\in L_2, \\ [u+d]\neq 0, x(0)=0}} \frac{\|y\|_2}{\|[u+d]\|_2}. \tag{2}$$

The operator $\|.\|_2$ denotes the standard L_2-norm for signals, i.e., $[\int_0^\infty u(t)^T u(t)\,\mathrm{dt}]^{\frac{1}{2}}$. A generalization of the Bounded Real Lemma (BRL) provides sufficient conditions to upper bound $\|P\|$ and can be found in [13].

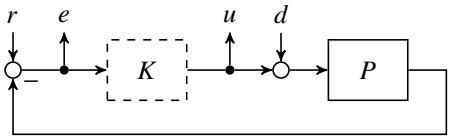

Fig. 1 Four-block mixed sensitivity problem.

In [12], the authors proposed a novel two step induced L_2 controller synthesis procedure for finite horizon LTV systems. This approach presents an alternative to classical LTP output feedback syntheses stated in, e.g., [14, Chapter 13.8.5]. These are also referred to as the periodic H_∞ problem. Fig. 1 shows the standard unity feedback control loop with time-varying plant P and time-varying controller K. Their closed interconnection is denoted by the lower fractional transformation $\mathcal{F}_l(P, K)$. The approach in [12] can be readily extended to synthesizes an LTP controller K

minimizing the induced L_2 norm of $\mathcal{F}_l(P,K)$:

$$\min_K \|\mathcal{F}_l(P,K)\|, \tag{3}$$

where K has the fixed structure

$$\left[\begin{array}{c}\dot{\xi}\\ \hline u\end{array}\right] = \left[\begin{array}{c|c} A(t)+B(t)F(t)+L(t)C(t) & L(t) \\ \hline F(t) & 0\end{array}\right]\left[\begin{array}{c}\xi\\ \hline e\end{array}\right]. \tag{4}$$

In (4), L is a time-periodic observer gain and F is a time-periodic state feedback gain. The gains follow from the solution of two unidirectionally coupled periodic Riccati differential equations provided in the following theorem under the assumption that the plant model (1) is strictly proper, i.e., $D = 0$, to simplify the notation. The theorem can be generalized to non-strictly proper plants at the cost of more complicated notation. However, usually engineering problems like wind turbines can be accurately represented by strictly proper models, e.g., by including actuator dynamics in the model.

Theorem 1 (Observer-Based Controller Synthesis) *Consider an LTP system* (1)*. There exists an observer-based controller K defined by (4) such that $\|\mathcal{F}_l(P,K)\| \leq \gamma$ iff the following two conditions hold.*

1) There exists a T-periodic, continuously differentiable, symmetric positive semi-definite matrix function $Z(t)$, $t \in [0,T]$ such that Z is a stabilizing solution to

$$\dot{Z} = AZ + ZA^T - ZC^T CZ + BB^T. \tag{5}$$

2) There exists a T-periodic continuously differentiable, symmetric positive semi-definite matrix function $X(t)$, $t \in [0,T]$ such that X is a stabilizing solution to

$$\dot{X} = -\bar{A}^T X - X\bar{A} + X\bar{T}X + C^T\bar{U}C, \tag{6}$$

with $\bar{A} = A - \frac{1}{1-\gamma^2}ZC^T$, $\bar{T} = \frac{1}{1-\gamma^2}ZC^TCZ + BB^T$, and $\bar{U} = \frac{\gamma^2}{1-\gamma^2}C^TC$.

Proof: The proof is analogous to the finite horizon LTV proof in [12] and thus omitted in this paper. □

The solution of the RDE (5) provides the periodic observer gain $L = -Z\,C^T$. In the same way, the solution of the RDE (6) provides the periodic state feedback gain $F = -B^T\,X$. Note that only the solution of the second RDE depends on γ. A bisection over γ repeatedly solving the second RDE (6) provides the minimal γ value. The solution of the corresponding RDE provides the optimal state feedback gain. The resulting L_2 optimal output feedback controller has the fixed structure given in Eq. (4).

Note that the proposed structured synthesis provides the exact same optimal L_2-norm as classical LTP output feedback syntheses (see e.g., [14]). However, the standard approaches require the solution of two bi-directionally coupled RDEs satisfying a spectral radius condition point-wise in time. Hence, two periodic Riccati differential equations have to be solved repeatedly. The spectral radius condition can only be checked after integration and potentially renders a solution invalid. These two characteristics create computational overhead, which is avoided by the structured control. Moreover, the classical approach provides a controller with no particular structure.

III. Structured Linear Time-Periodic Wind Turbine Control Design

The utility-scale three-bladed Clipper Liberty 2.5 MW wind turbine is investigated above rated wind speed, i.e., within operating region 3 in which the generator provides its maximum torque and maximum rotor speed needs to be tracked via blade pitching. Due to the high wind speeds, this region is the most critical one regarding the turbine's loads. While rotor speed tracking is generally achieved via collective pitching the blades, load reduction is enabled via individual blade pitching, stating a MIMO control problem. Classically, the resulting control problems are solved via decoupled control approaches using linear approximations of the turbine dynamics. With the design approach presented in Section II the periodic characteristics of the turbine can not only be fully exploited, but both control problems can be solved within a single control design directly.

A high-fidelity nonlinear framework of the Clipper wind turbine is available with the *Fatique, Aerodynamics, Structures and Turbulence* (FAST) simulation environment documented in [15]. The modes considered in the nonlinear simulation include first and second flapwise-blade bending, edgewise-blade bending, the first bending of the tower in

fore-aft and side-to-side direction, as well as generator speed and drive-train rotational flexibility. The model allows individual input for each blade-pitch angle and generator torque. The corresponding actuators are approximated as linear first-order systems with time constant $T = 0.1$ s. The provided nonlinear model includes a baseline controller that generates collective blade-pitch and torque commands based on the current rotor speed and provides baseline performance data, respectively. Numerous utility algorithms are provided within the FAST software, e.g., to linearize the nonlinear wind turbine model around the rotary trajectory.

A. Synthesis Model

FAST's internal linearization algorithms are used to calculate a gridded LTP model for the periodic controller synthesis. The algorithms linearize the open-loop nonlinear wind turbine dynamics without the baseline controller and actuator dynamics for a given wind speed. A constant wind speed of 20 m/s is used as reference wind speed. Located on the middle of the region 3 operation which reaches from 12 m/s to 25 m/s, at this wind speed the turbine is operated at its maximum reference rotor speed of $\omega_{\mathrm{R,\,ref}}$ of 15.6 rpm $\approx$ 1.62 rad/s. This corresponds to a period time T of 3.87 s. Here, FAST generates an LTP model with sixty grid points, which corresponds to a step sized of approximately 0.0645 s. This grid density accurately covers the wind turbines dynamics over one period as required for the synthesis. The calculated LTP system has an order of seven and includes the generator speed ω_{G} and the first flap-wise bending mode for each blade as states. The states are selected to enable a control design to meet the objectives of reference tracking and out-of-plane bending moment damping. The system's outputs are the three root out-of-plane bending moments $M = [M_1, M_2, M_3]^T$ at each blade together with the rotor speed ω_R. The system input is the individual blade-pitch command $\phi = [\phi_1, \phi_2, \phi_3]^T$ for each of the three blades, i.e., the rotational deflection of the rotor blades and a collective blade-pitch command ϕ_{coll}. For the synthesis, the individual pitch command signals are connected to the actuator dynamics. This ensures that the system shows no feed-through, i.e., $D = 0$, as required by Theorem 1. The input signal to of the synthesis model is therefore the commanded individual actuator pitch deflections. Extending the LTP model with the actuator dynamics increases the total number of the synthesis model states to ten.

B. Control Objectives and Choice of Weights

A specifically parameterized four-block mixed sensitivity formulation is used which facilitates transparent tuning based on given control objectives. Fig. 2 shows a graphical representation of the chosen closed loop synthesis structure, which follows the physical interpretable frequency dependent weights and scaling factors proposed in [10, 16]. This

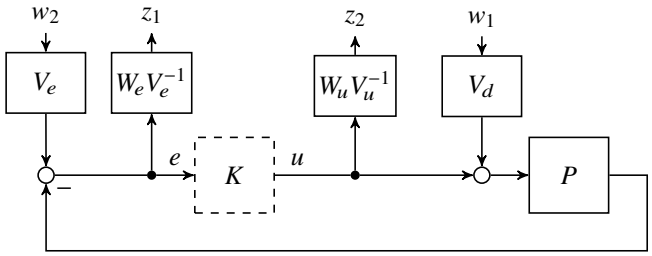

Fig. 2 Weighted four-block mixed sensitivity problem.

particular synthesis structure characterizes the control objectives in form of an induced L_2 norm optimization of the weighted closed-loop with the associated controller synthesis problem:

$$\min_K \left\| \begin{bmatrix} W_e V_e^{-1} & 0 \\ 0 & W_u V_u^{-1} \end{bmatrix} \begin{bmatrix} -SP & S \\ -KSP & KS \end{bmatrix} \begin{bmatrix} V_d & 0 \\ 0 & V_e \end{bmatrix} \right\|_{\infty}. \tag{7}$$

In Eq. (7), $S = (I + PK)^{-1}$ denotes the output sensitivity function [17], W_e and W_u frequency dependent weights and V_d, V_u, and V_e static scaling factors. Essentially, Eq. (7) is a weighted form of the mixed sensitivity problem introduced in Section II and can be solved for LTP systems by Theorem 1. The choice of weights and scaling factors is informed by requirements such as disturbance attenuation levels, tracking capabilities, the frequency range of control activity and robustness.

Specifically for the wind turbine control, each weighting and scaling has block diagonal structure. The weighting filter W_e shapes the scaled sensitivity function $V_e^{-1}SV_e$ and the scaled disturbance sensitivity function $V_e^{-1}SPV_d$. The entries in W_e correspond to the three blade bending moments and the rotor speed in this order. Tracking capability, i.e., a low magnitude of S, is only required for the latter. Hence, the rotor speed channel weight $W_{e,4}$ has integral behaviour up to a specified tracking bandwidth $\omega_{\text{bw}} = 2$ rad/s and magnitude 0.5 beyond this frequency. The bending moment channels have a constant magnitude of 0.5. The choice of 0.5 restricts the maximum peak magnitude of S to 2, which is a common requirement for robustness. Thus, W_e has the form

$$We(s) = \begin{bmatrix} 0.5I_{3\times3} & \\ & \frac{s+\omega_{\text{bw}}\sqrt{3/(1-\epsilon^2)}}{2s+\epsilon\omega_{\text{bw}}\sqrt{3/(1-\epsilon^2)}} \end{bmatrix}, \tag{8}$$

where the off-diagonal elements are omitted to facilitate readability and $\epsilon \ll 1$. The scaling factors V_e and V_d are chosen based on the maximum allowable error and the maximum expected disturbance, respectively. The scaling $V_e = \text{diag}(40, 40, 40, 0.5)$ which corresponds to maximum bending moment errors of 40 kNm and a maximum rotor speed error of 0.5 rpm. The disturbance scaling is 1 degree in all channels, i.e. $V_d = I_{4\times4}$. The constant scaling for the disturbance sensitivity function in the bending moments enforces a load reduction over a broad frequency range.

The weighting filter W_u shapes the scaled control sensitivity $V_u^{-1}KSV_e$ and therefore determines the frequency range of control activity. Since IPC is used exclusively for load reduction, whereas CPC tracks the rotor speed, the control authority is separated in two distinct frequency ranges, one for IPC and the other for collective pitch. The chosen parametrization of W_u is

$$W_{u,1}(s) = W_{u,2}(s) = W_{u,3}(s) = \frac{s+\omega_{l,\text{IPC}}}{s+0.01\omega_{l,\text{IPC}}}\left(\frac{0.1s+\omega_{h,\text{IPC}}}{s+\omega_{h,\text{IPC}}}\right)^2, \tag{9}$$

$$W_{u,4}(s) = \frac{0.1s+\omega_{h,\text{CPC}}}{s+\omega_{h,\text{CPC}}}, \tag{10}$$

and $W_u = \text{diag}(W_{u,1}, W_{u,2}, W_{u,3}, W_{u,4})$. Here, $\omega_{l,\text{IPC}}$ and $\omega_{h,\text{IPC}}$ set the lower and upper limit for the control bandwidth of the individual pitch commands. They are set to 3.5 rad/s and 5.5 rad/s, respectively. This choice restricts the IPC to only work in the bandwidth of the blade bending mode and not interfere with the tracking of the rotor speed at low frequencies, nor command blade pitch beyond the actuator bandwidth. The collective pitch channel only has an upper limit of $\omega_{h,\text{CPC}} = 3$ rad/s. Hence, it restricts the collective pitch to tracking rotor speed at low frequencies. The scaling V_u is consequently set to represent the maximum available control action in relation to the previously specified control error V_e and disturbance V_d. A value of 2 deg is selected for all channels, i.e., $V_u = 2I_{4\times4}$.

C. LTP Controller Synthesis and Implementation

Using the weights provided in the previous section and the LTP representation of the wind turbine the structured LTP controller is synthesized. First, the observer gain L is calculated by solving a scaled version of the periodic RDE (5). This scaled RDE can be readily derived following the step by step explanations in [16]. It is solved forward in time over three periods for zero initial conditions using the Matlab solver `ODE15s` [18]. This approach allows the solution to converge to the stabilizing periodic solution and takes 1.23 s on a standard desktop PC. The last period of the RDE solution is used to calculate the observer gain. Next, the state feedback synthesis is conducted using L in an augmented version of the state feedback RDE (6). Matlab's `ODE15s` solves this RDE backwards in time for zero initial conditions over six periods repeatedly in a bisection over γ. The bisection calculates the minimal feasible γ of 5.9 in 14.41 s. This γ value is the optimal solution of the output feedback problem (7). Again, the last period is used to calculate the state feedback gain. In total, the controller synthesis requires approximately 15.64 s.

Finally, the structured LTP controller is assembled from the calculated observer and state feedback gain, the plant and weighting filters and scaling factors in accordance to Fig. 3, where A_{W_e}, B_{W_e}, A_{W_u}, and B_{W_u} represent the state space matrices of the respective weighting filter. The controller dynamics consist of three elements with clear interpretations. The first element, *Integral Augmentation*, contains the integral rotor speed tracking. The second dynamic part is the *Luenberger Observer*. The third dynamic element, namely *Control Effort Filter*, provides the additional user-specified control limitations, i.e. bandpass for IPC and roll-off for collective pitch. Selective channels of the resulting controller at different times are shown in Fig. 4. The integral action in the rotor speed to collective pitch command channel, i.e., K_{44}, is clearly visible, as is the bandpass characteristics in the bending moment to individual blade pitch command. The

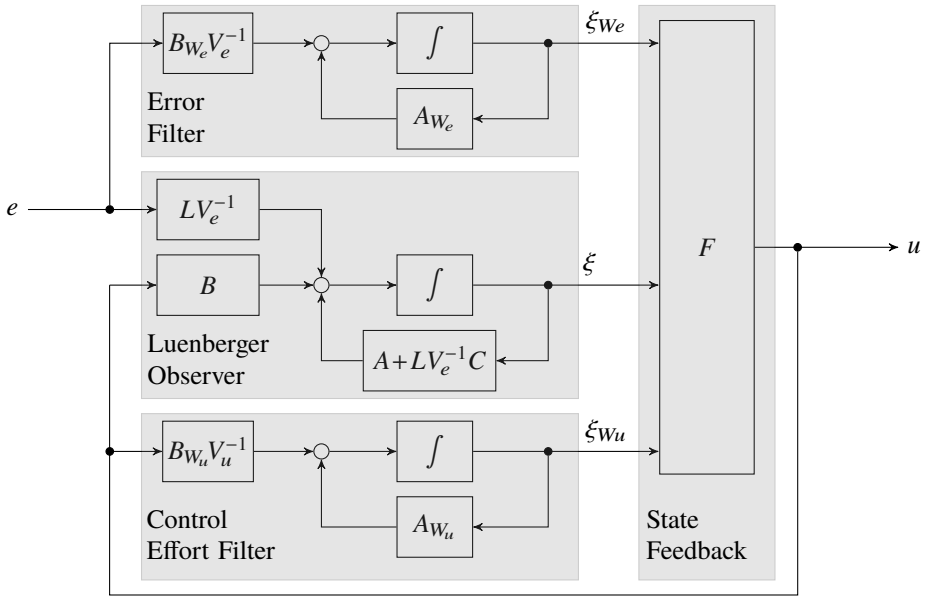

Fig. 3 Observer-based controller including weights.

latter is shown on the example of blade one, i.e., K_{11}. The other blade channels show a similar behaviour. Note that due to the chosen scaling factors the bandpass is at a higher frequency than the weight might suggest. The off diagonal channels in the IPC have much lower gains than the diagonal which is to be expected, see e.g., K_{21} in the figure.

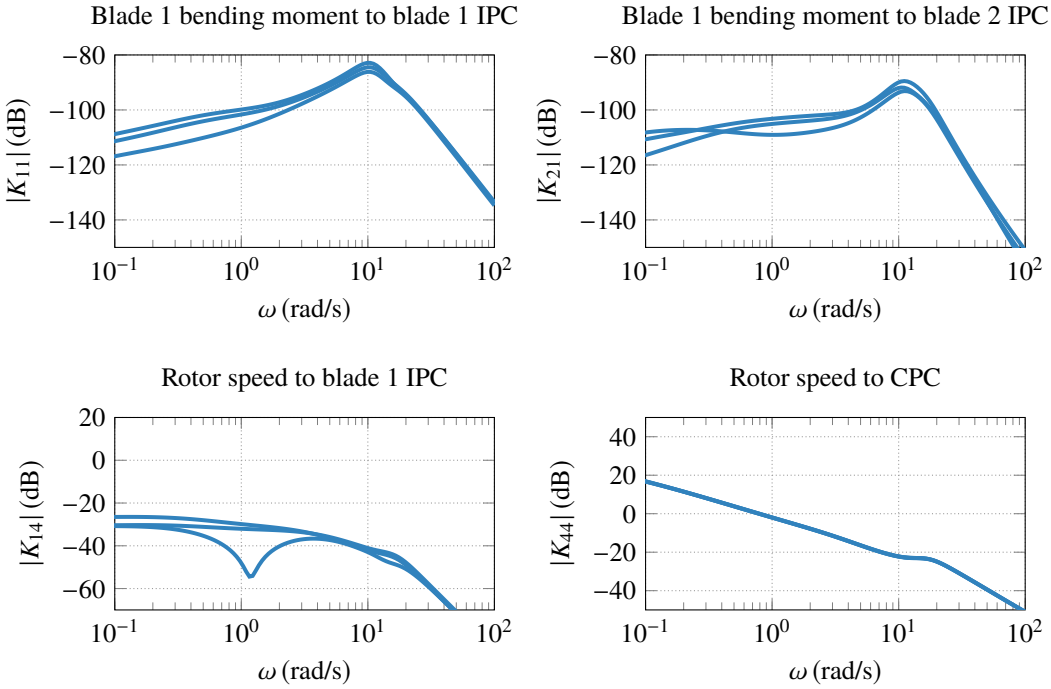

Fig. 4 Selected controller transfer functions for 0 s, 1.25 s, and 2.56 s along the period.

The effective load reduction is showcased in Fig. 5, which compares the disturbance sensitivity function with the open loop disturbance response for the bending moment of the first blade. It can be seen that the controller is reducing the effects of disturbances on bending moments over a wide frequency range. At low frequencies the effect diminishes due to the bandpass of the IPC.

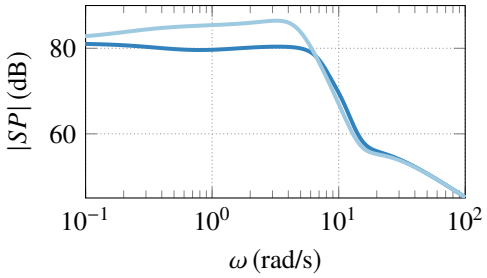

Fig. 5 Disturbance open loop response (——) and closed loop (——) blade pitch to bending moment at 1.9 s.

Although, the controller is synthesized with a dependence on time, time does not present the most suitable scheduling parameter for implementation. The obvious practical reasons are non-nominal rotational speeds and thus period times caused by wind disturbances. It is possible to replace time with an alternative scheduling parameter. Such a parameter must be strictly periodic so that a one-on-one map to time exists. A suitable choice for scheduling is the rotor angle $\Psi(t) \in [0, 2\pi]$. For implementation, the synthesis time grid and the corresponding controller dynamics are mapped onto the nominal rotor angle profile. The rotor angle is then used as scheduling signal in the nonlinear simulation.

IV. Controller Verification

The performance of the LTP controller is evaluated using a nonlinear simulation model of the Clipper turbine in the software environment FAST. Two control strategies, representative of the current industrial standard, are used for comparison. The first control strategy is a baseline controller that includes protection functions. This controller tracks the generator's speed in region 3, however, it does not offer any additional load reduction capabilities. In the second reference scenario, the baseline controller is augmented with an individual blade-pitch controller. This classical individual blade-pitch controller consists of two decoupled SISO integral compensators with an open-loop bandwidth of approximately 0.25 rad/s to compensate for the yawing and pitching in the fixed coordinate frame caused by the interactions of the three blades, see [19]. Consequently, the controller, along with the MBC-transformation and its inverse, is implemented to transform the available blade loads into the fixed frame, process the result signals through the controller, and transform the generated commands back to actual blade pitch commands in the rotary frame. Further details on this controller can be found in [4].

For a realistic verification, the control strategies are compared under turbulent wind conditions of class A, as specified by the *International Electrotechnical Comission* (IEC). The 10 minutes log turbulent wind field is generated using the TURBSIM software with the Kaiman Model as the turbulence spectral model. The mean hub height wind speed is set to 20 m/s, corresponding to the operating condition selected in Section III. The resulting rotor speed tracking performance of the turbine is visualized in Fig. 6 for a four minute snapshot of the ten minute simulation. Note that the red line indicates the rotor speed tracking target of 15.6 rpm. A comparison of the baseline controller with the augmented baseline controller reveals that the two SISO loops for load reduction do not interfere with the rotor speed tracking at all. The controller proposed herein exhibits slightly better damping in the rotor speed tracking behavior. The

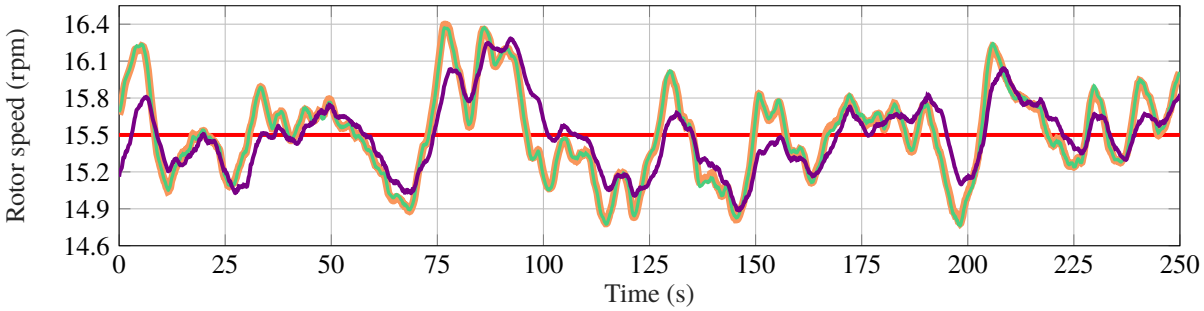

Fig. 6 Rotor speed in turbulent wind conditions with baseline controller (——), the augmented baseline controller with two SISO integral loops (——), and the LTP controller (——).

generated power for the turbine results from the multiplication of the generated rotor speed with the moment on the generator. A deeper analysis shows that all three controllers ensure a time averaged power output of 2.5 MW over the 10 minute simulation time. For the LTP controller the increased damping already indicates the presence of improved load reduction compared to the augmented baseline controller.

To verify the load reduction as well as the required control activity, the results from the simulations with the turbulent wind field are further evaluated. This evaluation is performed via computing the frequency-dependent power spectral density (PSD) of the out-of-plane bending moments at the blade root as well as the realized pitch angles by the actuators. Fig. 7 illustrates the corresponding power spectral densities (PSDs) for the first blade. Results only for the first blade are presented, since the behavior of all three blades is very similar. In the left diagram, the baseline controlled system (—) shows a dominant peak of blade loads around the 1P frequency at 0.258 Hz, simply resulting from the rotation of the turbine. The augmented baseline controller (— is able to clearly reduce those so-called 1P moments but has no significant impact on the moments at other frequencies. This reduction at the 1P frequency results from the explicit targeting of these 1P moments via the MBC transformation together with the two integral control loops [19]. In contrast, the LTP controller (—) effectively reduces the moment magnitudes over a broad frequency band up to around 0.9 Hz due to the chosen roll-off frequency (at 5.5 rad/s ≈ 0.87 Hz). However, it does not explicitly target the 1P frequency so that only a small reduction of the 1P moments compared to the augmented controller is achieved. Correspondingly, the overall pitch activity of the LTP controlled system above the 1P frequency is higher than the pitch activity of the augmented baseline controlled system, while the latter shows a dominant peak at the 1P frequency. This is illustrated via the corresponding PSDs of the blade pitch motion in the right diagram of Fig. 7. Note that the blade pitch PSD of the LTP controller is not reduced directly after 0.9 Hz. The increased pitch activity up to about 2 Hz results from the peak in the controller gains as shown in Fig. 5. As they do not show an effect on the loads, the weighting could be further adjusted that this unnecessary actuator activity is reduced in future implementations.

Finally, to be able to strengthen the statement that the LTP controller reduces the loads better than the classical approach with two integral control loops, a statistical analysis on the so-called Damage Equivalent Loads (DELs) is performed. The DELs represent a measure of equivalent fatigue damage caused by each load and take into account material properties [19]. They can be computed based on simulation output data from FAST using the software tool MCrunch [20]. While the DELs for the blades are computed for obvious reasons, the DELs are also computed for the tower, the generator shaft, and the nacelle to get a clearer picture of the performance of the proposed controller. Remember, none of these loads should drastically increase due to adverse coupling when introducing the additional load reduction capabilities. For the material properties, in this work, S-N slopes of 4 for the tower, shaft and nacelle, and 10 for the blades are used, representative of typical steel and composite materials. To enable the statistical analysis, 20 unique wind signals are generated by using unique random seeds for the turbulence, each 10 minutes long. Fig. 8 shows the resulting statistical evaluation of the generated DELs using box-plots. Therein the box itself contains 50% of the gathered data points. The black horizontal lines represent the median value. The ends of the whiskers of each box are defined by the lowest data point still within 1.5 times the interquartile range of the lower quartile and the highest data

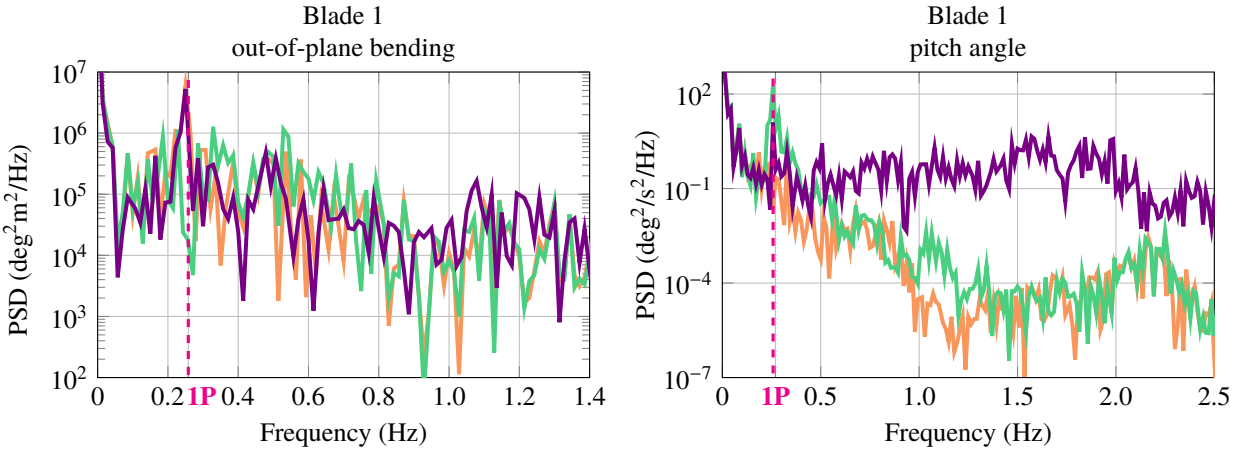

Fig. 7 PSDs of the first blades out-of-plane bending moment and pitch activity for the baseline controller (—), the augmented baseline controller with two integral SISO loops (—), and the LTP controller (—).

point still within 1.5 times the interquartile range of the upper quartile [21]. All box plots are normalized with respect to the median DELs that occur with the baseline controller to enable an easy comparison. For the blades, again only the results of the first blade are shown.

The primary target of the control design is the reduction of the out-of-plane bending moments acting on the blade root. The statistical analysis of the DELs for these out-of-plane bending shows that the explicit reduction of the 1P moments by the augmented baseline controller leads to a mean reduction by about 15 %. The reduction of all moment magnitudes over a broader bandwidth by the LTP controller is slightly better and achieves a mean reduction by about 18 %. Note that this is achieved although the 1P frequency is not explicitly targeted. Additionally, the LTP controller, also enables a reduction of the in-plane bending DELS at the blade roots of about 5 % while the augmented baseline controller reduces the mean by only 1-2 %. The LTP controller reduces the DELs of the shaft bending by about 18 % while the augmented baseline controller increases them slightly by 1.5 %. The better performance of the baseline controller results from the load reduction capabilities at higher frequencies, as only those higher frequencies influence the DELs in the fixed, i.e, non rotary, frame. This is also confirmed when analyzing the nacelle loads . Here the LTP controller reduces the pitch and yawing moments on the nacelle by about 20 % each. Due to the missing pitching action of the augmented controller at higher frequencies, these loads are barely effected by this controller, even showing a slight increase in nacelle yawing DELs of about 2 % and nacelle pitching DELs of about 3 %.

Shaft torque DELs remain largely unaffected by the augmented controller, while the LTP controller increases the shaft torque by about 10 %. This is a consequence of the high frequency pitch activity, visible in the analysis of the pitch activity in Fig. 7. This also leads to the increase in the tower side-to-side DELs, as those high-frequency torque moments directly couple with the tower side-to-side motion. In contrast, the augmented baseline controller achieves a reduction of 6.5 % of the tower side-to-side DELs. This is achieved as the IPC is able to reduce the blades' in-plane moments, which directly couple with the tower side-to-side motion. Note, that the LTP controller also reduces the blades' in-plane moments. Still, shaft torque and tower side-to-side DELs increase, as the controller injects high-frequency

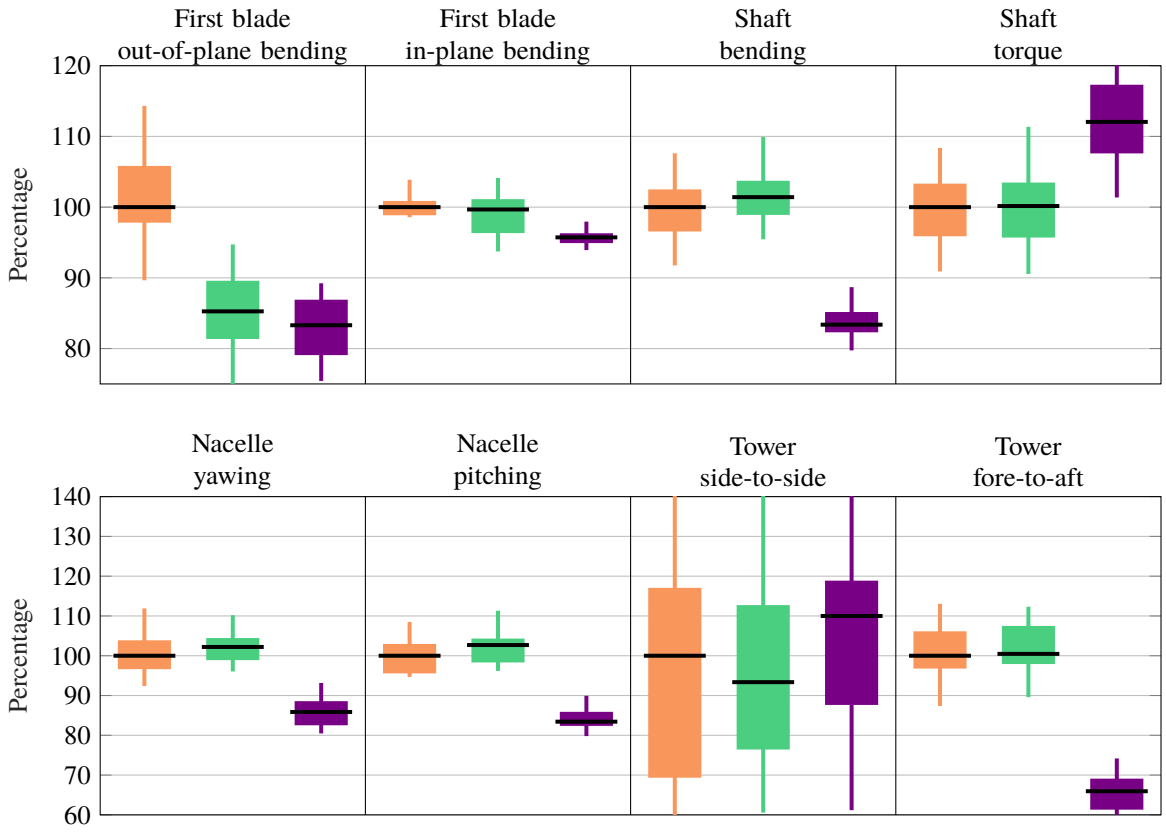

Fig. 8 Statistical evaluation of DELs for the baseline controller (—), the augmented baseline controller (—), and the LTP controller (—).

collective pitch motion to enable improved rotor speed tracking. Thus, regarding shaft torsion and tower side-to-side DELs, the positive effect of reduced in-plane moments is eaten up by the negative effect of high frequency collective pitch commands, injecting adverse loading on those two component directions. Finally, due to the reduction of the out-of-plane moments over a broad frequency band, the LTP controller achieves a 35 % reduction of the tower fore-to-aft DELs. Those loads are barely effected by the augmented controller due to its low bandwidth.

Based on the discussions above it can be concluded that the LTP controller provides substantial load reduction while achieving good rotor speed tracking accuracy. Moreover, the mixed sensitivity based synthesis facilitates an intuitive design and tuning process to trade off between these two requirements.

V. Conclusion

The present paper showcases the advantages of a direct robust periodic control design for a utility-scale wind turbine. By avoiding coordinate transformations and averaging, the performance of individual pitch controllers can be significantly improved. A novel structured robust controller synthesis approach is used which offers an intuitive design process. It facilitates the transfer of the method into an industrial setting which requires versatility and ease of controller tuning. A complete evaluation of the control design is be performed in form of a probabilistic performance analysis. The verification campaign demonstrates that an individual pitch control strategy which exploits the wind turbines periodic dynamics can provide significant load reduction together accurate rotor speed tracking.

References

[1] Orell, A., Kazimierczuk, K., and Sheridan, L., "Wind Market Reports: 2022 Edition," *Pacific Northwest National Laboratory*, 2022.

[2] Donham, R. E., and Heimbold, R. L., "WIND TURBINE," , 1979. Patent 4,297,076.

[3] Bossanyi, E. A., Fleming, P. A., and Wright, A. D., "Validation of Individual Pitch Control by Field Tests on Two- and Three-Bladed Wind Turbines," *IEEE Transactions on Control Systems Technology*, Vol. 21, No. 4, 2013, pp. 1067–1078. doi:10.1109/TCST.2013.2258345.

[4] Ossmann, D., Seiler, P., Milliren, C., and Danker, A., "Field Testing of Multi-Variable Individual Pitch Control on a Utility-Scale Wind Turbine," *Renewable Energy*, Vol. 170, 2021, pp. 1245–1256. doi:10.1016/j.renene.2021.02.039.

[5] Ossmann, D., Theis, J., and Seiler, P., "Load reduction on a clipper liberty wind turbine with linear parameter-varying individual blade pitch control," *Wind Energy*, Vol. 20, No. 10, 2017, pp. 1771–1786. doi:110.1002/we.2121.

[6] Bir, G., *User's Guide to MBC3: Multi-Blade Coordinate Transformation Code for 3-Bladed Wind Turbines*, National Renewable Energy Laboratory, Golden, Colorado, USA, 2010. NREL/TP-500-44327.

[7] Jakobsen, C. S., Camino, J. F., and Santos, I., "Rotor-Blade Vibration Control Using a Periodic LQR Controller," *Proceeding Series of the Brazilian Society of Applied and Computational Mathematics*, Vol. 1, No. 1, 2013. doi:10.5540/03.2013.001.01.0011.

[8] Camino, J. F., and Santos, I. F., "A periodic linear–quadratic controller for suppressing rotor-blade vibration," *Journal of Vibration and Control*, Vol. 25, No. 17, 2019, pp. 2351–2364. doi:10.1177/107754631985335.

[9] Thiele, F., Wisbacher, S., Diaconescu, S.-M., Ossmann, D., and Pfifer, H., "Periodic LQG Wind Turbine Control with Adaptive Load Reduction," *22nd IFAC World Congress*, 2023. doi:10.1016/j.ifacol.2023.10.1168.

[10] Theis, J., Pfifer, H., and Seiler, P., "Robust Modal Damping Control for Active Flutter Suppression," *J. Guidance, Control, Dynamics*, Vol. 43, No. 6, 2020, pp. 1056–1068. doi:10.2514/1.g004846.

[11] Burgin, E., Biertümpfel, F., and Pfifer, H., "Linear Parameter Varying Controller Design For Satellite Attitude Control," *IFAC World Congress*, 2023. doi:10.1016/j.ifacol.2023.10.1443.

[12] Biertümpfel, F., Theis, J., and Pfifer, H., "Observer-Based Synthesis of Finite Horizon Linear Time-Varying Controllers," *2022 American Control Conference (ACC)*, IEEE, 2022. doi:10.23919/acc53348.2022.9867184.

[13] Colaneri, P., "Continuous-time periodic systems in H_2 and H_∞ Part I: Theoretical Aspects," *Kybernetika*, Vol. 36, No. 2, 2000, pp. 211–242.

[14] Bittanti, S., and Colaneri, P., *Periodic Systems*, Springer London, 2009. doi:10.1007/978-1-84800-911-0.

[15] Jonkman, J. M., and Buhl, M. L., *FAST User's Guide*, National Renewable Energy Laboratory, Golden, CO, USA, Oct. 2005. NREL/TP-500-38230.

[16] Theis, J., and Pfifer, H., "Observer-based synthesis of linear parameter-varying mixed sensitivity controllers," *Int. J. Robust Nonlinear Control*, Vol. 30, No. 13, 2020, pp. 5021–5039. doi:10.1002/rnc.5038.

[17] Green, M., and Limebeer, D. J. N., *Linear Robust Control*, Prentice-Hall, Inc., Upper Saddle River, NJ, USA, 1995.

[18] MATLAB, *R2020b*, The MathWorks Inc., Natick, Massachusetts, 2020.

[19] Bossanyi, E. A., "Individual Blade Pitch Control for Load Reduction," *Wind Energy*, Vol. 6, 2003, pp. 119–128. doi: 10.1002/we.76.

[20] Buhl, M., *MCrunch User's Guide for Version 1.00*, National Renewable Energy Laboratory, Golden, CO, USA, May 2008. NREL/TP-500-43139.

[21] Frigge, M., Hoaglin, D. C., and Iglewicz, B., "Some implementations of the boxplot," *The American Statistician*, Vol. 43, No. 1, 1989, pp. 50–54.